Hindawi Publishing Corporation
Journal of Nanotechnology
Volume 2014, Article ID 474909, 7 pages
http://dx.doi.org/10.1155/2014/474909

Research Article

Synthesis, Characterization, and Magnetic Studies of α-Fe_2O_3 Nanoparticles

Avnish Kumar Arora,[1] Mohan Sharma,[1] Ritu Kumari,[1] Vivek Sheel Jaswal,[1] and Pankaj Kumar[2]

[1] *Department of Chemistry, Maharishi Markandeshwar University, Mullana, Haryana 133207, India*
[2] *Department of Chemistry, College of Engineering Studies, University of Petroleum and Energy Studies, Bidholi, Dehradun 248001, India*

Correspondence should be addressed to Avnish Kumar Arora; aroradcy@gmail.com

Received 27 May 2013; Revised 19 November 2013; Accepted 19 November 2013; Published 29 January 2014

Academic Editor: Paresh Chandra Ray

Very fine nanosized metal oxide, namely, iron oxide (α-Fe_2O_3) has been synthesized by precipitation method using ammonia as precipitating agent and characterized by using XRD (X-ray diffraction), TGA/DTA, surface area measurement, transmission electron microscopy (TEM), and magnetic measurements techniques. XRD studies show that iron oxide was formed as α-Fe_2O_3 instead of the commonly formed magnetite nanoparticles (Fe_3O_4) or a mixture of magnetite (Fe_3O_4) and maghemite (γ-Fe_2O_3, cubic), and it has rhombohedral structure. Magnetic measurements showed that iron oxide has five unpaired electrons and is ferromagnetic in nature, Ms value being 1.7 emu/g. The particle size of the synthesized iron oxide was determined by TEM. TEM images show that the size of particles of Fe_2O_3 varied from 15 nm to 49 nm with average crystallite size 35 nm.

1. Introduction

Transition metal oxides have many applications as catalysts [1–5], sensors [6–9], superconductors [10, 11], and adsorbents [12, 13]. Metal oxides constitute an important class of materials that are involved in environmental science, electrochemistry, biology, chemical sensors, magnetism, and other fields. One of their most important applications is heterogeneous catalysis. Iron oxides belong to the most abundant minerals and occur with a large variety of stoichiometries, structures, and properties. The more important ones are FeO (wustite), λ-Fe_2O_3 (maghemite), α-Fe_2O_3 (hematite), and Fe_3O_4 (magnetite) with rock-salt, vacancy rich inverse spinel, corundum, and inverse spinel structures, respectively; the two former ones being thermodynamically less favorable and α-Fe_2O_3 being the most oxidized one. Iron oxides are widely used in industry as catalysts or catalyst supports. Nanosized iron oxide particles within various ordered mesoporous silicas (SBA-15, SBA-16, Fm3m, and Ia3d) have been prepared from the corresponding nitrate and acetylacetonate precursors and studied for their catalytic behavior in methanol decomposition [14]. Nanosized catalyst (iron oxide) into the pores of a mesoporous material (titania) has been deposited using ultrasound radiation and the resulting catalyst is used for the oxidation of cyclohexane under mild conditions [15]. Nanosized iron and mixed iron-cobalt oxides supported on activated carbon materials and their bulk analogues have been synthesized and their catalytic behavior in methanol decomposition to H_2, CO, and methane is tested [16]. A series of nanosized gold/iron-oxide catalysts has been prepared and tested for CO oxidation [17]. Catalytic oxidation of PCDD/Fs (polychlorinated dibenzo-*p*-dioxins and polychlorinated dibenzofurans) with ozone (catalytic ozonation) over nanosized iron oxides (denoted as Fe_xO_y) has been carried out at temperature of 120–180°C [18]. Iron oxide nanoparticles (IOnPs) as solid catalyst were prepared using a biotic method, that is, biomineralization, and abiotic methods, that is, thermal decomposition and electrochemical methods, for use as solid catalysts in the heterogeneous catalytic ozonation of *para*-chlorobenzoic acid (*p*CBA) [19]. Nanosized iron oxide has applications in waste water treatment and as sensors. Role of nanosized colloidal iron oxides in microbial iron reduction has been studied [20]. Implications of heat treatment on the

properties of a magnetic iron oxide-titanium dioxide photocatalyst have been studied [21]. Nanosized iron oxide particles were intercalated into the interlayer of layered compounds $HTiNb(Ta)O_5$ by a successive ion-exchange reaction and studied for photocatalytic water splitting [22]. Adsorption and desorption properties of arsenate [As (V)] on nano-sized iron-oxide-coated quartz (IOCQ) through batch experiments were conducted to investigate the coating of nano-sized iron oxide on the quartz surface using the heat treatment process which aimed to utilize the adsorption properties of the nano-sized iron oxide and the filtration properties of the quartz [23]. Removal of phosphate from solution using nanosized FeOOH-modified anion resin was studied in fixed bed column. Effect of bed height and flow rate on the breakthrough curves was investigated [24]. Nanosized particles of α-Fe_2O_3 in the range of 17–64 nm were synthesized and were used for LPG sensing [25]. A simple and reproducible method to obtain TiO_2 and Fe_2O_3 mixed oxide thin films by reactive RF sputtering has been presented and investigated for the gas sensing properties toward CO [26]. Different methods have been used for the synthesis of nanosized iron oxide nanoparticles. The raw material Lauha churna (iron filings) that has been taken as raw material for the synthesis of nanosized iron oxide and phase transformation from α- to γ-phase has been studied [27]. Highly crystallized iron oxide nanorods have been fabricated by hydrothermal synthesis in the cavity of carbon-coated nanochannels with a diameter of 25 nm [28]. Nanosized iron oxide powder with average crystallite sizes 35, 100 and 150 nm was prepared by thermal evaporation and coprecipitation techniques and tested as catalyst for the photocatalytic decomposition of Congo red dye [29]. Nanosized iron oxides have considerable attention due to their unique magnetic properties (superparamagnetism, high coercivity, low curie temperature, high magnetic susceptibility, nontoxicity, biocompatibility, and low cost of production), which allow their usage in various nanotechnology applications in a broad range of disciplines. Magnetic nanoparticles are also important in biomedical applications, for example, magnetic bioseparation [30], magnetic target drug delivery [31], hyperthermia [32], magnetic resonance imaging [33], and magnetofection [34]. In the present paper we have synthesized α-Fe_2O_3 nanoparticles by simple aqueous precipitation using ammonia as precipitating agent and their magnetic properties have been studied. This method involves a simple, cheap, and one-step process for synthesis of Fe_2O_3 nanoparticles. Iron oxide was formed as α-Fe_2O_3 instead of the commonly formed magnetite nanoparticles (Fe_3O_4) or a mixture of magnetite (Fe_3O_4) and maghemite (γ-Fe_2O_3, cubic). The obtained particles of Fe_2O_3 have size from 15 to 42 nm. The synthesized nanoparticles were characterized by XRD, TGA/DTA, magnetic susceptibility, and TEM.

2. Methods and Materials

2.1. Chemicals. All chemicals used in the experiment are analytic reagent grade. Ferric nitrate, $Fe(NO_3)_3$, was purchased from Merck, India. Ammonium hydroxide (liquor ammonia) was purchased from SRL. Deionized water was used throughout the experiment.

2.2. Synthesis of Iron Oxide. 500 mL of 0.1 M solution of $Fe(NO_3)_3$ was taken and aqueous ammonia was added dropwise with constant stirring until the pH of the solution reached 10. The precipitates thus obtained were filtered by Buckner funnel and were washed several times with distilled water. The precipitates were dried in oven at 70°C for 24 hrs and were calcined at 500°C in a muffle furnace for 5 hrs. Obtained material was ground and sieved through 100 mesh size sieve.

2.3. Characterization Techniques. The microstructure of the particles was characterized by X-ray diffraction (XRD), Philips PW 11/90 diffractometer using nickel filtered CuKα (l = 1.5405 Å) radiations. The average diameter (D) of the iron oxide nanocrystals has been calculated from the broadening of the XRD peak intensity after Kα_2 corrections using the Debye-Scherrer equation. Transmission electron microscopy (TEM) measurements of the sample were taken on Hitachi H7500 with a 70 kV accelerating voltage. The dispersions of nanoparticles in water were placed on carbon-coated 400 mesh copper grids, allowed to dry at room temperature before taking measurement. The obtained micrographs were then examined for particle size and shape. The magnetic property of the solid was measured at 300 K using a Vibrating sample Magnetometer Model 155. TGA/DTA studies were carried out using Perkin Elmer Pyris Diamond. The BET surface area of the samples was measured by nitrogen adsorption isotherms on micromeritics ASAP 2010 (UK).

3. Results and Discussions

3.1. X-Ray Studies. X-ray diffraction of synthesized oxide is shown in Figure 1. X-ray diffraction pattern of pure iron oxide indicated that iron oxide was in the form of α-Fe_2O_3 (Figure 1). The X-ray diffraction plot, shown in Figure 1, shows peaks only due to α-Fe_2O_3 and no peak is detected due to any other material or phase indicating a high degree of purity of the as-synthesized sample. The broadening of the X-ray diffraction lines, as seen in the figure, reflects the nanoparticle nature of the sample. In X-ray diffraction, some prominent peaks were considered and corresponding d-values were compared with the standard [JCPDS file no. 85-0987] (Table 1). X-ray diffraction shows that metal oxide is pure α-Fe_2O_3 having rhombohedral structure.

Sharpness of the peaks shows good crystal growth of the oxide particles. Average particle size (t) of the particles has been calculated from high intensity peak using the Debye-Scherrer equation

$$t = \frac{K\lambda}{B\cos\theta}, \tag{1}$$

where t is the average crystallite size of the phase under investigation, K is the Scherrer constant (0.89), λ is the wave length of X-ray beam used, B is the full width at half

Table 1: X-ray diffraction data for iron oxide (α-Fe_2O_3).

S. No.	d (Å) (observed)	d (Å) (reported)	$I/I_0 \times 100\%$ (observed)	$I/I_0 \times 100\%$ (reported)
(1)	3.6806	3.6775	35.78	58.7
(2)	2.6980	2.6959	100.00	100
(3)	2.5155	2.5135	83.14	63.1
(4)	2.2033	2.2015	24.03	3.4
(5)	1.8394	1.8379	36.98	6.1
(6)	1.6949	1.6936	43.26	18.0
(7)	1.4852	1.4840	26.88	18.1
(8)	1.4511	1.4512	26.77	9.7

85–0987 Wavelength= 1.54060 C

Fe_2O_3

Iron Oxide

Haematite

Rad.: CuKa1 λ: 1.54060 Filter: d–sp: Calculated

Cut off: 17.7 Int.: Calculated I/Icor.: 4.00

Ref: Calculated from ICSD using POWD–12++, (1997)

Ref: Zachariasen, W.H., Skr. Nor. Vidensk.–Akad., Kl. 1: Mat.–Naturvidensk. Kl., 1928, 1 (1928)

Sys.: Rhombohedral S.G.: R$\bar{3}$c (167)

a: 5.42(2) b: c: A: C: 1.0000

α: 55.200(1) β: γ: Z: 2 mp:

Ref: Ibid.

Dx: 5.302 Dm: ICSD # : 033643

Peak height intensity. R–factor: 0.081. Al2 03 type. C.D. Cell: a=5.022, c=13.738, c/a=2.7354, S.G.=R–3c(167). PSC: hR10. Mwt: 159.69. Volume[CD]: 300.07.

2θ	Int	h	k	l	2θ	Int	h	k	l
24.201	587	1	1	0	84.578	5	4	4	4
33.212	999*	1	2	1	85.191	57	3	2	1
35.729	631	1	1	0	88.440	4	1	4	0
39.320	334	2	2	2	88.808	57	2	4	0
40.957	34	1	2	0					
43.622	3	0	2	0					
49.575	61	2	2	0					
54.168	180	1	3	2					
56.319	7	1	2	0					
57.609	27	1	2	1					
57.609		3	3	2					
62.598	181	1	3	0					
64.191	97	2	1	1					
66.194	3	2	3	0					
69.720	27	2	4	2					
72.035	75	3	4	3					
75.361	3	2	4	1					
75.690	76	2	2	0					
77.936	56	3	3	0					
79.014	1	1	3	1					
79.738	2	2	2	1					
80.835	18	1	3	0					
80.835		3	4	1					
83.094	18	2	4	4					

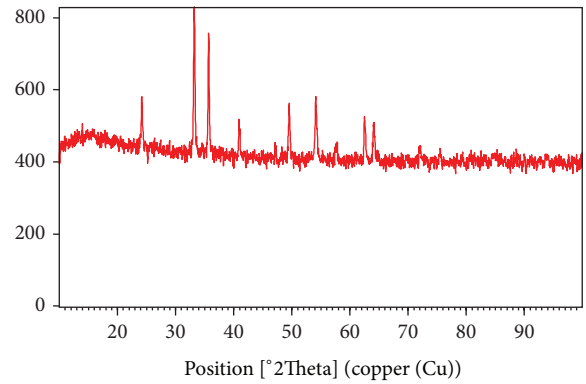

Figure 1: -XRD spectra of synthesized iron oxide.

maximum (FWHM) of diffraction (in radians), and θ is the Bragg's angle.

The average crystallite size calculated is 35 nm which is in close agreement with the TEM results.

3.2. Magnetic Measurements. The magnetic moment for iron oxide was carried out at room temperature and was observed as 5.68 B.M. This value of magnetic moment supports the fact that the synthesized iron oxide is in the form of Fe_2O_3 with actual magnetic moment 5.92 B.M. This indicates the presence of 5 unpaired electrons in Fe_2O_3. Magnetic measurements were also carried out at temperatures ranging from 300 K to 100 K to determine the temperature of Morin transition. The results are shown in Figure 2(a) and have been reported in Table 2. VSM studies were carried out at 300 K to show hysteresis behavior of nanosized particles and it has

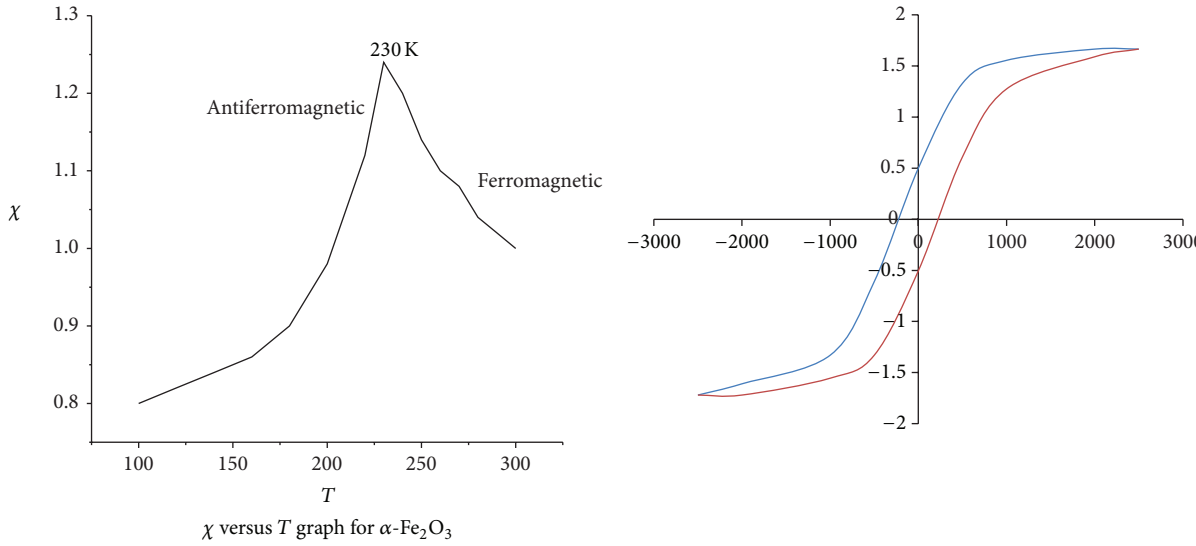

Figure 2: (a) Morin transition curve for synthesized iron oxide nanoparticles. (b) VSM studies of synthesized iron oxide.

Table 2: Magnetic susceptibility data of iron oxide.

Temperature (K)	Volt (mV)	Magnetic moment (emu.)
300	5.75	0.0050
290	5.58	0.0051
280	5.38	0.0052
270	5.17	0.0054
260	4.96	0.0055
250	4.75	0.0057
240	4.54	0.0060
230	4.33	0.0062
220	4.13	0.0056
200	3.71	0.0049
180	3.29	0.0045
160	2.88	0.0043
140	2.46	0.0042
120	2.05	0.0041
100	1.63	0.0040

been observed that Fe_2O_3 show ferromagnetic behavior in nanocrystalline form, Ms value being 1.7 emu/g (Figure 2(b)).

3.3. TGA/DTA Studies. TGA/DTA transition shows an endothermic peak at 364°C (Figure 3). It simply indicates that when FeO(OH) is heated, it takes an amount of energy and 1.5 water molecules are removed. So, for the formation of iron oxide temperature above 364°C is required.

3.4. Surface Area Measurement. The BET surface area of the samples was measured by nitrogen adsorption isotherms. Surface area of the metal oxide was 27 m^2/g. Samples were activated at 473 K for 4 h prior to the measurement.

3.5. TEM Studies. TEM studies were carried out to find out exact particle size of synthesized Fe_2O_3. Figure 4 shows the

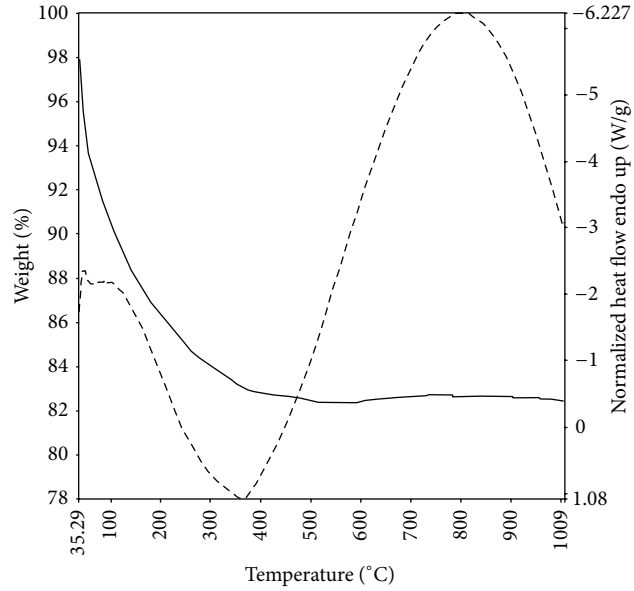

Figure 3: TGA/DTA curve of iron oxide heated at 70°C.

TEM image of the synthesized Fe_2O_3 nanoparticles. TEM images show that Fe_2O_3 nanoparticles are having particle size in the range of 15 nm–49 nm (Figure 4). The size distribution histograms for nanoparticles provided their respective sizes as 29.8 ± 8.4 nm (Figure 4(a)), 30.6 ± 7.0 nm (Figure 4(b)), 26.4 ± 4.7 nm (Figure 4(c)), and 32.4 ± 6.6 nm (Figure 4(d)), respectively.

4. Conclusion

α-Fe_2O_3 nanoparticles with rhombohedral structure are synthesized successfully by aqueous precipitation method using ammonia as precipitating agent. From TEM study, it is found

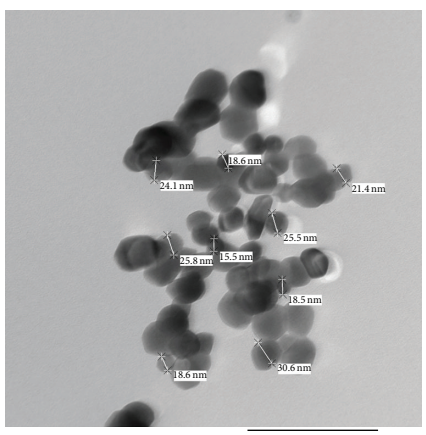

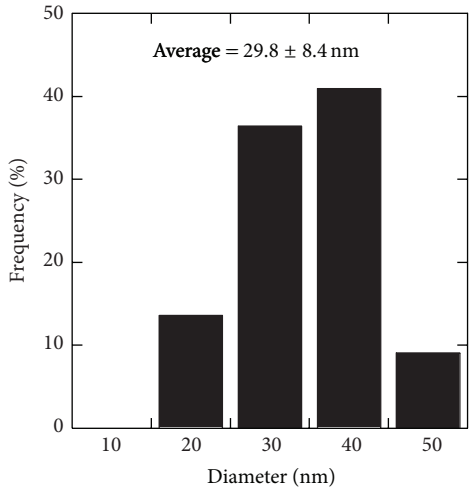

(a)

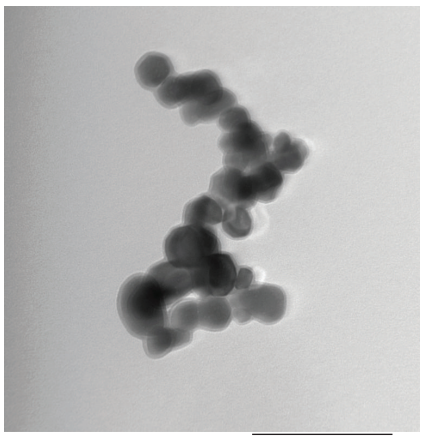

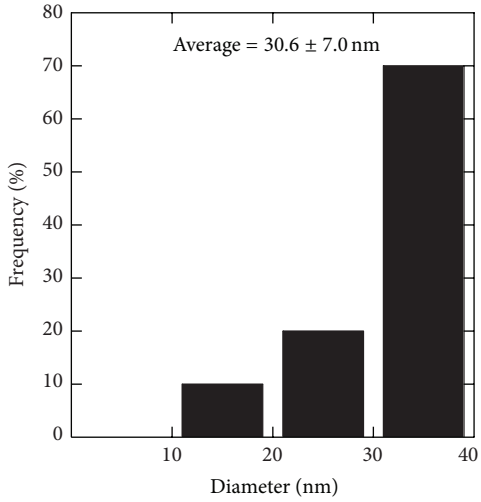

(b)

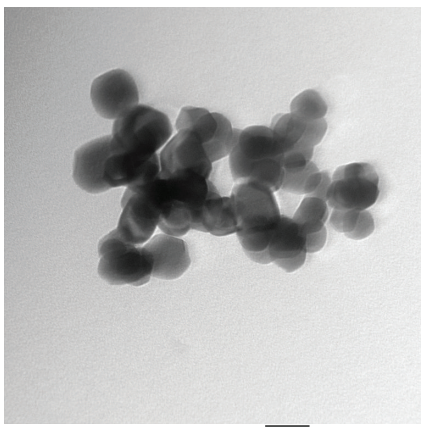

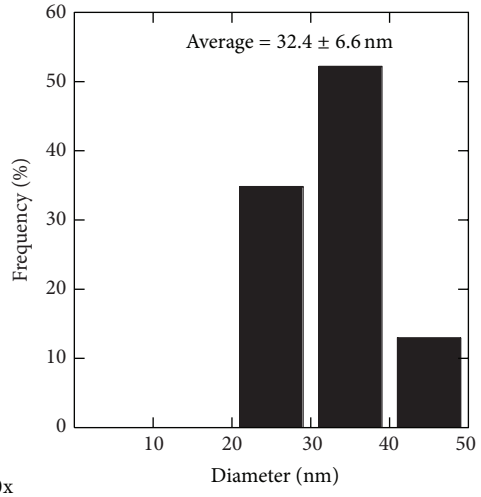

(c)

Figure 4: Continued.

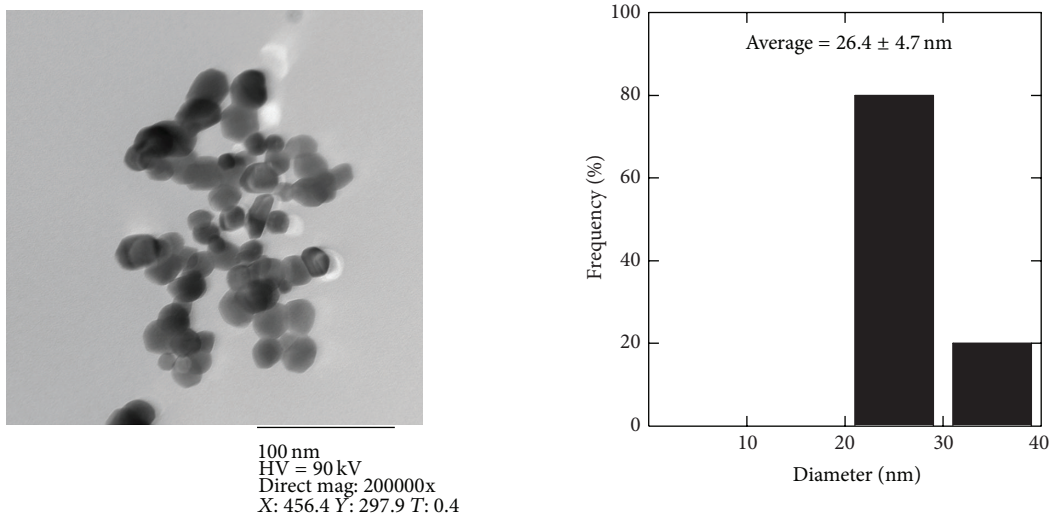

(d)

Figure 4: TEM images of iron oxide particles.

that particles are with average size of 15–49 nm. Magnetic measurements show that Fe_2O_3 has five unpaired electrons. VSM studies show ferromagnetic behavior of synthesized oxides. XRD studies show that iron oxide was formed as α-Fe_2O_3 instead of the commonly formed magnetite nanoparticles Fe_3O_4 or a mixture of magnetite and maghemite.

Conflict of Interests

The authors declare that there is no conflict of interests regarding the publication of this paper.

References

[1] J. Z. Xu, J. J. Zhu, H. Wang, and H. Y. Chen, "Nano-sized copper oxide modified carbon paste electrodes as an amperometric sensor for amikacin," *Analytical Letters*, vol. 36, no. 13, pp. 2723–2733, 2003.

[2] W. Z. Lv, B. Liu, Z. K. Luo, X. Z. Ren, and P. X. Zhang, "XRD studies on the nanosized copper ferrite powders synthesized by sonochemical method," *Journal of Alloys and Compounds*, vol. 465, no. 1-2, pp. 261–264, 2008.

[3] H. C. Lu, J. L. Lu, C. L. Chu, C. Y. Lai, and G. M. Wu, "Preparation of nano-powders of p-type transparent conductive copper aluminum oxide by co-precipitation method," in *Proceedings of the 2nd IEEE International Nanoelectronics Conference (INEC '08)*, pp. 485–488, Shanghai, China, March 2008.

[4] T. G. Altinçekiç, I. Boz, and S. J. Aktürk, "Synthesis and characterization of nanosized Cu/ZnO catalyst by polyol method," *Journal of Nanoscience and Nanotechnology*, vol. 8, no. 2, pp. 874–877, 2008.

[5] S. Bennici, A. Gervasini, and V. Ragaini, "Preparation of highly dispersed CuO catalysts on oxide supports for de-NO(x) reactions," *Ultrasonics Sonochemistry*, vol. 10, no. 2, pp. 61–64, 2003.

[6] M. Yang, J. He, X. Hu et al., "Copper oxide nanoparticle sensors for hydrogen cyanide detection: unprecedented selectivity and sensitivity," *Sensors and Actuators B*, vol. 155, no. 2, pp. 692–698, 2011.

[7] H. Wei, H. Sun, S. Wang et al., "Low temperature H_2S sensor based on copper oxide/tin dioxide thick film," *Journal of Natural Gas Chemistry*, vol. 19, no. 4, pp. 393–396, 2010.

[8] G. An, Y. Zhang, Z. Liu et al., "Preparation of porous chromium oxide nanotubes using carbon nanotubes as templates and their application as an ethanol sensor," *Nanotechnology*, vol. 19, no. 3, Article ID 035504, 2008.

[9] S. S. Sharma, K. Nomura, and Y. U. Ujihira, "Characterization of tin oxide films prepared as gas sensors by conversion electron Mössbauer spectrometry," *Journal of Materials Science*, vol. 26, no. 15, pp. 4104–4109, 1991.

[10] V. Pillai, P. Kumar, M. J. Hou, P. Ayyub, and D. O. Shah, "Preparation of nanoparticles of silver halides, superconductors and magnetic materials using water-in-oil microemulsions as nanoreactors," *Advances in Colloid and Interface Science*, vol. 55, pp. 241–269, 1995.

[11] R. Wu, J. Qu, H. He, and Y. Yu, "Preparation and characterization of Cu catalysts supported on organized mesoporous alumina," *Journal of Beijing University of Chemical Technology (Natural Science Edition)*, vol. 48,, pp. 2311–2316, 2003.

[12] W. Zou, R. Han, Z. Chen, J. Shi, and L. Hongmin, "Characterization and properties of manganese oxide coated zeolite as adsorbent for removal of copper(II) and lead(II) ions from solution," *Journal of Chemical and Engineering Data*, vol. 51, no. 2, pp. 534–541, 2006.

[13] R. Han, L. Zou, X. Zhao et al., "Characterization and properties of iron oxide-coated zeolite as adsorbent for removal of copper(II) from solution in fixed bed column," *Chemical Engineering Journal*, vol. 149, no. 1–3, pp. 123–131, 2009.

[14] T. Tsoncheva, J. Rosenholm, C. V. Teixeira, M. Dimitrov, M. Linden, and C. Minchev, "Preparation, characterization and catalytic behavior in methanol decomposition of nanosized iron oxide particles within large pore ordered mesoporous silicas," *Microporous and Mesoporous Materials*, vol. 89, no. 1–3, pp. 209–218, 2006.

[15] N. Perkas, Y. Wang, Y. Koltypin, A. Gedanken, and S. Chandrasekaran, "Mesoporous iron-titania catalyst for cyclohexane oxidation," *Chemical Communications*, no. 11, pp. 988–989, 2001.

[16] E. Manova, T. Tsoncheva, C. Estournès et al., "Nanosized iron and iron-cobalt spinel oxides as catalysts for methanol decomposition," *Applied Catalysis A*, vol. 300, no. 2, pp. 170–180, 2006.

[17] N. A. Hodge, C. J. Kiely, R. Whyman et al., "Microstructural comparison of calcined and uncalcined gold/iron-oxide catalysts for low-temperature CO oxidation," *Catalysis Today*, vol. 72, no. 1-2, pp. 133–144, 2002.

[18] H. C. Wang, S. H. Chang, P. C. Hung, J. F. Hwang, and M. B. Chang, "Catalytic oxidation of gaseous PCDD/Fs with ozone over iron oxide catalysts," *Chemosphere*, vol. 71, no. 2, pp. 388–397, 2008.

[19] H. Jung, H. Park, J. Kim et al., "Preparation of biotic and abiotic iron oxide nanoparticles (IOnPs) and their properties and applications in heterogeneous catalytic oxidation," *Environmental Science and Technology*, vol. 41, no. 13, pp. 4741–4747, 2007.

[20] J. Bosch, K. Heister, T. Hofmann, and R. U. Meckenstock, "Nanosized iron oxide colloids strongly enhance microbial iron reduction," *Applied and Environmental Microbiology*, vol. 76, no. 1, pp. 184–189, 2010.

[21] D. Beydoun and R. Amal, "Implications of heat treatment on the properties of a magnetic iron oxide-titanium dioxide photocatalyst," *Materials Science and Engineering B*, vol. 94, no. 1, pp. 71–81, 2002.

[22] J. S. Jang, H. G. Kim, V. R. Reddy, S. W. Bae, S. M. Ji, and J. S. Lee, "Photocatalytic water splitting over iron oxide nanoparticles intercalated in HTiNb(Ta)O_5 layered compounds," *Journal of Catalysis*, vol. 231, no. 1, pp. 213–222, 2005.

[23] M. G. Mostafa, Y. H. Chen, J. S. Jean, C. C. Liu, and H. Teng, "Adsorption and desorption properties of arsenate onto nano-sized iron-oxide-coated quartz," *Water Science and Technology*, vol. 62, no. 2, pp. 378–386, 2010.

[24] N. Li, J. Ren, L. Zhao, and Z. L. Wang, "Fixed bed adsorption study on phosphate removal using nanosized FeOOH-modified anion resin," *Journal of Nanomaterials*, vol. 2013, Article ID 736275, 5 pages, 2013.

[25] B. C. Yadav, S. Singh, A. Yadav, and T. Shukla, "Experimental investigations on nanosized ferric oxide and its LPG sensing," *International Journal of Nanoscience*, vol. 10, no. 1-2, pp. 135–139, 2011.

[26] E. Comini, V. Guidi, C. Frigeri, I. Riccò, and G. Sberveglieri, "CO sensing properties of titanium and iron oxide nanosized thin films," *Sensors and Actuators B*, vol. 77, no. 1-2, pp. 16–21, 2001.

[27] T. Pavani, C. S. Chakra, and K. V. Rao, "A Green approach for the synthesis of nano-sized iron oxide, by Indian ayurvedic modified bhasmikaran method," *The American Journal of Biological, Chemical and Pharmaceutical Sciences*, vol. 1, no. 1, pp. 1–7, 2013.

[28] K. Matsui, T. Kyotani, and A. Tomita, "Hydrothermal synthesis of nano-sized iron oxide crystals in the cavity of carbon nanotubes," *Molecular Crystals and Liquid Crystals Science and Technology A*, vol. 387, no. 2, pp. 1–5, 2002.

[29] M. H. Khedr, K. S. Abdel Halim, and N. K. Soliman, "Synthesis and photocatalytic activity of nano-sized iron oxides," *Materials Letters*, vol. 63, no. 6-7, pp. 598–601, 2009.

[30] S. L. Miller and L. E. Orgel, *The Origins of Life on Earth*, Prentice Hall, Englewood Clifts, NJ, USA, 1974.

[31] M. Paecht-horowitz, J. Berger, and A. Katchalsky, "Prebiotic synthesis of polypeptides by heterogeneous polycondensation of amino-acid adenylates," *Nature*, vol. 228, no. 5272, pp. 636–639, 1970.

[32] J. Wang, Z. Zhu, A. Munir, and H. S. Zhou, "Fe_3O_4 nanoparticles-enhanced SPR sensing for ultrasensitive sandwich bioassay," *Talanta*, vol. 84, no. 3, pp. 783–788, 2011.

[33] J. Chomoucka, J. Drbohlavova, D. Huska, V. Adam, R. Kizek, and J. Hubalek, "Magnetic nanoparticles and targeted drug delivering," *Pharmacological Research*, vol. 62, no. 2, pp. 144–149, 2010.

[34] C. S. S. R. Kumar and F. Mohammad, "Magnetic nanomaterials for hyperthermia-based therapy and controlled drug delivery," *Advanced Drug Delivery Reviews*, vol. 63, no. 9, pp. 789–808, 2011.